

INFLUENCE OF THE TYPE OF DEFORMATION AND TEXTURE ON THE DAMAGEABILITY AND MECHANICAL PROPERTIES OF ZE10 MAGNESIUM ALLOY

V. V. Usov,^{1,2} N. M. Shkatulyak,¹ O. S. Savchuk,³ and N. I. Rybak¹

UDC 539.32

We study the effects of extrusion treatment with subsequent rolling in combination with annealing, changes in the direction of rolling after each pass (original sheet), and alternating bending (AB) for 0.5; 1; 3, and 5 cycles, as well as the effect of texture on the parameter of damage D and the elastic and mechanical properties of the material in uniaxial tensile tests (ultimate strength σ_u , yield point $\sigma_{0.2}$, and relative elongation Δ/l) for the ZE10 magnesium alloy with zinc, zirconium, and rare-earth metals.

We determined the values of damage parameters according to the changes in the modulus of elasticity after the corresponding number of AB cycles relative to its values in different directions for the original analyzed sheet. Note that the damage parameters were computed by using the models of equivalent strains and equivalent elastic energy. It is established that the elasticity moduli, ultimate strengths, conventional yield points, and relative elongations averaged over all directions in the sheets of the alloy, decrease and, on the contrary, the corresponding values of damage parameters increase with the number of AB cycles and obey parabolic laws, as follows from the correlation and regression analyses. The anisotropy of indicated characteristics also weakens under the conditions of alternating bending. It was also shown that there exist strong correlation relations between the Kearns texture parameters, on the one hand, and the moduli of elasticity, damage parameters, ultimate strengths, yield points, and relative elongation, on the other hand. We deduce the corresponding quadratic regression equations with high values of the reliability index of approximation. It was also shown that the indicated changes in the analyzed properties are mainly caused by the variations of crystallographic textures.

Keywords: extrusion, rolling, alternating bending, texture, anisotropy, elasticity modulus, damage parameter, correlation.

Introduction

Magnesium and its alloys are promising materials, in particular, for the automotive and aerospace industries due to their low density and high specific strength [1]. As the main disadvantage of pure magnesium and some of its alloys, e.g., AZ31 alloy (that contains aluminum, zinc, and zirconium), we can mention their low susceptibility to form changes under high strains [2]. Moreover, magnesium, as the major part of metals with hexagonal crystal structures is characterized by a noticeable anisotropy of the mechanical properties caused by the formation of undesired textures, which restricts the possibilities of its practical application. Magnesium and its alloys are deformed according to numerous mechanisms of slip (basic, prismatic, and pyramidal) and with the help

¹ K. Ushynskiy South-Ukrainian National Pedagogical University, Odessa, Ukraine.

² Corresponding author; e-mail: valentinusov67@gmail.com.

³ “Odessa Marine Academy” National University, Odessa, Ukraine.

of certain types of twinning. The mechanisms of deformation depend on the ratio of the parameters of crystal structure c/a [3]. As a result of the proper alloying of magnesium in the course of production of the alloys, we can obtain new materials with a certain complex of required properties including, in particular, stable corrosion resistance and good susceptibility to form changes.

As shown earlier, the addition of rare-earth metals (REM) to Mg alloys weakens their texture in the course of rolling or extrusion as compared with the other magnesium alloys. To explain this phenomenon, a series of mechanisms was proposed in [4–6]. Thus, in [7], it was shown that minor admixtures of REM not only decrease sharpness of texture but also promote the elevation of plasticity and corrosion resistance of magnesium alloys.

As a rule, prior to application, sheet and coiled metals are straightened in special straighteners by alternating bending (AB). After this treatment, we obtain plane sheets with low levels of residual stresses [8]. Under the conditions of AB, the material undergoes insignificant alternating deformation, which leads to certain changes in the texture and microstructure [9].

At the same time, the damageability of sheets of ZE10 alloy obtained as a result of deformation by means of extrusion and subsequent rolling (with changes in its direction after each pass) in combination with annealing and alternating bending has not been studied earlier.

As already indicated, it is customary to apply AB in order to get better flatness and decrease residual stresses in the sheet metal prior to its application. In this case, in the process of deformation, the following types of sub- and microdefects are accumulated in the metal: point (vacancies and inclusions), linear (dislocations), surface (submicrocracks), and volume (micropores). The phenomenon of merging of these defects observed as deformation increases promotes the formation of microcracks. Joining into a single main crack, they may lead to the final fracture of the product [10, 11].

For the description of the macroscopic behavior of materials in the process of deformation, it is possible to use a promising concept of damage accumulation from the mechanics of continua. To characterize process of damage accumulation, we use the so-called damage parameter D proposed in [10, 11] and developed up to now [12–14]. The value of the damage parameter $0 \leq D \leq 1$ characterizes the entire set of microstructural changes in the material caused by the formation and accumulation of microdefects under the action of working loads. It is interpreted as the relative decrease in the effective load-carrying cross-sectional area caused by the accumulation of defects. The degradation of the material is caused by the gradual decrease in its effective area that, in fact, carries the load in tension and specifies the tensile strength of the specimen:

$$D = \frac{S - S_0}{S_0}, \quad (1)$$

where S_0 and S are, respectively, the cross-sectional areas of the intact and damaged specimens and $S_0 - S$ is the area occupied by the microcavities and microcracks.

For this interpretation, the damage parameter can be found according to the changes in the modulus of elasticity. According to the hypothesis of equivalent strains [12], the damage parameter D_1 can be found as follows:

$$D_1 = 1 - \frac{E}{E_0}, \quad (2)$$

where E_0 and E are the elasticity modulus of the intact specimen and the current value of this modulus, respectively.

If we use the model of equivalent elastic energy [13], then we can find D_2 as a fourth-rank tensor as follows:

$$D_2 = 1 - \left(\frac{E}{E_0} \right)^{1/2}. \quad (3)$$

Under uniaxial tension [11], only one component of the tensor in relation (3) differs from zero. The damage parameter D can be found in the case of uniaxial tension according to the changes in the elastic characteristics, with regard for the representative volume element of the orthotropic symmetry. We keep in mind that the orthotropic anisotropy is the most complicated type of anisotropy. Even in the case of high density of interacting cracks, the effective elastic properties remain orthotropic with good accuracy [10]. The damage parameter based on the Lemaitre model of equivalent strains [9] takes higher values as compared with the models of equivalent elastic energy [13, 14], which give very close numerical values [15]. Therefore, the values of the damage parameter D_2 estimated by using relation (3) are better as compared with the value given by (2) for the analysis of the anisotropy of damage to the sheet material [15].

The crystallographic texture formed under the conditions of plastic deformation also exerts a significant influence on the accumulation of structural defects and, hence, on the degree of damage [16]. However, the absence of an adequate physical substantiation of the models (kinetic equations) leads to ambiguities in the experimental evaluation of the damage parameter D depending on the method of its determination for the same sample of the analyzed material [15]. Hence, the relationship between the damage parameter and the variations of structural state of the material and its texture under the action of external factors can still be obtained only on the basis of the corresponding correlation and regression analyses.

The aim of the present work is to investigate the influence of extrusion with subsequent rolling and alternating bending and texture on the damage parameter D and elastic and mechanical properties of the material in uniaxial tensile tests (ultimate strength σ_u , yield point $\sigma_{0.2}$, and relative elongation $\Delta l/l$) for the ZE10 magnesium alloy with additions of zinc, zirconium, and REM.

Material and Methods of Investigation

Sheets of ZE10 alloy [1.3% Zn, 0.15% Zr, and 0.2% REM (mainly cerium)] were obtained as a result of treatment [17], including the procedure of extrusion of ingots at a temperature of 350°C as a result of which we obtained a slab with a thickness of 6 mm and a width of 60 mm. Then the slab was successively rolled in the longitudinal direction down to a thickness of 4.5 mm in two passes combined with heating up to 350°C after each pass. The subsequent rolling to a thickness of 2 mm was performed in the transverse direction in combination with heating to 350°C after each pass. The degree of straining in each pass was ~ 10%. Starting from a thickness of 2 mm, we changed the direction of rolling by 90° after each pass with a degree of straining of ~ 10% combined with heating to 350°C. In this way, we obtained sheets with a thickness of 1 mm (original sheets).

The process of alternating bending was modeled by using a hand-held bending instrument with three rolls \varnothing 50 mm. The velocity of motion of the metal bending was ~ 150 mm/sec. The experiments were carried out after 0.5; 1; 3, and 5 cycles. A single AB cycle consisted of bending in one direction (0.25 cycle) followed by straightening to the plane state (0.5 cycle), bending in the opposite direction (0.75 cycle), and final straightening.

Young's modulus was measured by using a dynamic method according to the frequency of natural bending vibration of plane specimens 100 mm in length and 10 mm in width cut out from the sheets at angles measured

with steps of 15° from the direction of rolling (RD) toward the transverse direction (TD). The error did not exceed 1% [17].

From the original sheet and sheets obtained after 0.5; 1; 3, and 5 cycles of bending, we cut out three batches of specimens for mechanical testing both in the RD and in the diagonal direction (DD), i.e., at an angle of 45° to the RD, and TD. Moreover, we also prepared the specimens for the investigation of texture.

The mechanical investigations were carried out in a Zwick Z250/SN5A tensile-testing machine with a force gauge on 20 kN at room temperature for specimens cut out in the RD, TD, and DD. The total length of the specimens was equal to 90 mm. The length and width of their working parts were 30 and 12.5 mm, respectively. As the values of mechanical characteristics, we took the results of measurements averaged over three series of tests in each direction.

Prior to the texture investigations, the specimens were chemically polished down to a depth of 0.1 mm in order to remove the distorted surface layer. The crystallographic textures were analyzed for two specimen surfaces after the indicated numbers of AB cycles by means of a survey of inverse pole figures both in the direction of normal (DN IPF) and in the direction of rolling (RD IPF) with the help of a DRON-3m diffractometer in the filtered MoK_α -radiation. A specimen without texture was prepared from fine recrystallized grains of the investigated alloy. In constructing the IPF, we used the Morris normalization [18].

Results and Discussion

In Fig. 1, we present the IPF for the investigated alloy. It is easy to see that the texture of original specimens of ZE10 alloy (Figs. 1a and b) is characterized by a wide prevailing scattering of normals to the basis planes in the TD with the maximal angle of deviation of 90° and intermediate maxima of deviation of the hexagonal prism from the DN both toward TD by 40° and to the side of RD by 40° , unlike the texture, which is, as a rule, formed in Mg, Ti, and Zr. The character of texture scattering and the pole density on the IPF of ZE10 alloy vary depending on the number of AB cycles (Figs. 1c–l). In a certain stage of AB, similar changes in texture serve as an indication of the deformation processes of slip and twinning [9]. For the numerical analysis of the textures of hexagonal materials, the researchers often use the so-called Kearns texture parameters [19]. These parameters f_j [the subscript j denotes the corresponding direction in the specimen (DN, RD, or TD)] indicate the degree of coincidence of the c -axes of the crystal hexagonal cell of grains with a given geometric direction in the polycrystalline material. They can be found from the IPF as follows:

$$f_j = \langle \cos^2 \alpha_i \rangle_j = \sum_i A_i P_{ji} \cos^2 \alpha_i, \quad (4)$$

where

$$P_{ji} = \frac{I_i/I_R}{\sum_{\Delta} (A_i \cdot I_i/I_R)},$$

I_i/I_R is the ratio of the integral intensity I_i of the i th reflex to the corresponding integral intensity I_R of the i th reflex of the specimen without texture on the j th IPF, and A_i are the statistical weights of the i th reflex ($\sum A_i P_{ji} = 1$) [18]. The value of A_i is conventionally determined as a part of the surface area of stereographic triangle around the normal and the i th reflex of the corresponding IPF, and α_i is the angle of deviation of the i th crystallographic direction from the c -axis for the j th direction in the specimen. To determine the Kearns

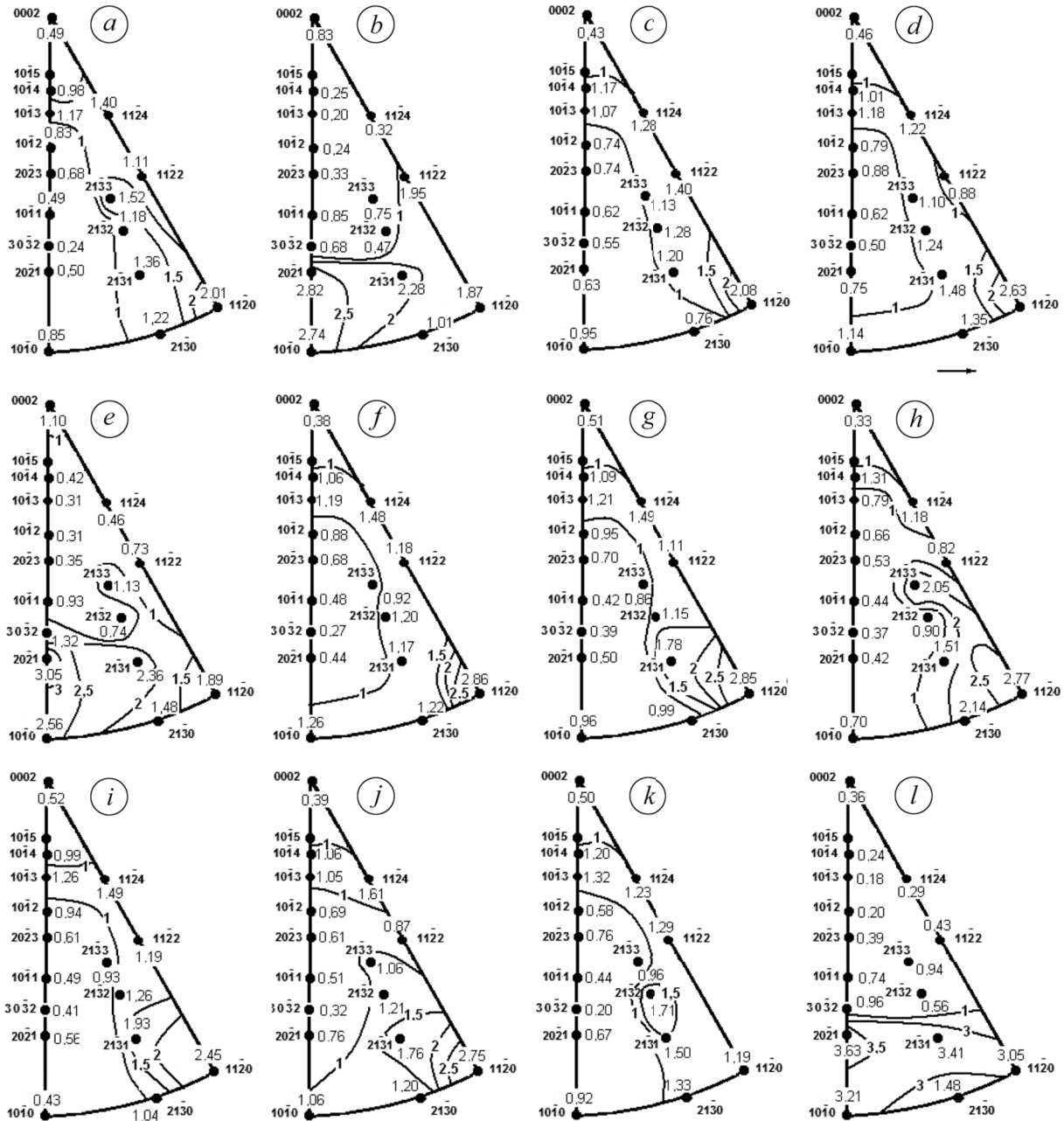


Fig. 1. Experimental inverse pole figures for ZE10 alloy: original sheet [(a) and (b)]; sheets subjected to alternating bending for 0.5 (c–e); 1 (f, g); 3 (h, i), and 5 (j–l) cycles; (b, e, and l) correspond to the direction of rolling; (a, c, d) and (f–k) correspond to the direction of normal to the rolling plane; (d, f, h, and j) correspond to the stretched side of the sheets, and (c, g, i, and k) correspond to their compressed side.

texture parameters, we used the IPF presented in Fig. 1 and the values were taken from [20]. To compute the angles α_i according to the well-known formulas from [21], it is necessary to know the ratio of the parameters of crystal lattice c/a for the analyzed alloy.

For the ZE10 magnesium alloy, we have $c/a = 1.622$. A similar result was also obtained in [22]. We revealed discrepancies between the distributions of pole density for the DN IPF of the opposite sides of sheets after the corresponding number of AB cycles (Figs. 1c, d, and f–k). This is explained by the fact that, on the convex

Table 1
Kearns Texture Parameters of the Sheets of ZE10 Alloy Computed According to the IPF Presented in Fig. 1

No. of cycles of alternating bending															
0		0.5				1			3			5			
f_{ND}	f_{RD}	f_{ND}^1	f_{ND}^2	f_{ND}^{av}	f_{RD}	f_{ND}^1	f_{ND}^2	f_{ND}^{av}	f_{ND}^1	f_{ND}^2	f_{ND}^{av}	f_{ND}^1	f_{ND}^2	f_{ND}^{av}	f_{RD}
0.340	0.176	0.322	0.324	0.323	0.203	0.322	0.318	0.320	0.326	0.306	0.316	0.323	0.315	0.319	0.153

side of the sheets, the surface layers are subjected to the action of tensile strains (Figs. 1d, f, h, and g), whereas the layers located on the opposite side suffer the influence of compressive strains (Figs. 1c, g, i, and k). Similar discrepancies were detected earlier [23] in analyzing the characteristics of crystallographic texture for the strips of Zr–2.5% Nb alloy cut out from the pipe and then straightened.

The revealed discrepancies between the distributions of pole density in the DN IPF for the opposite sides of the sheets of analyzed alloy corresponding to different numbers of AB cycles naturally affect the corresponding Kearns texture parameters (Table 1). The Kearns texture parameters f_{ND} of the original sheet of investigated alloy and also the parameters averaged over two sides of the sheets f_{ND}^{av} after different numbers of AB cycles were used for the subsequent analysis of the relationship between their values and the values of Young's modulus E , ultimate strength, yield point, relative elongation, and damage parameters D_1 and D_2 [computed according to relations (2) and (3), respectively] averaged over all directions in the sheets.

The elasticity moduli E , damage parameters D_1 and D_2 , ultimate strengths σ_u , yield points $\sigma_{0.2}$, and relative elongations $\Delta l/l$ for various directions of the original sheet and sheets of the analyzed alloy subjected to different numbers of AB cycles and also the values of the corresponding anisotropy factors η are summarized in Tables 2–7. The anisotropy factors were determined as follows:

$$\eta = \left[\frac{F_{\max} - F_{\min}}{F_{\min}} \right] \cdot 100\%, \quad (5)$$

where F is the value of corresponding characteristic.

Hence, the elasticity modulus is anisotropic both in the original sheet of the investigated alloy and after alternating bending. The degree of anisotropy is maximal in the original sheet (7.4%). As the number of AB cycles increases, the degree of anisotropy decreases, and its minimal value (5.4%) is attained after 5 AB cycles (Table 3). The averaged moduli of elasticity E decrease from 44 GPa in the original sheet to 43.2 GPa after 5 AB cycles (Table 2). The performed analysis revealed the existence of correlation between the elasticity modulus E_{av} averaged over directions and the number n of AB cycles. The corresponding regression equation and the reliability index of the approximation R^2 have the form:

$$E_{av} = 0.05n^2 - 0.38n + 43.96, \quad R^2 = 0.95. \quad (6)$$

For the investigation of the influence of alternating bending on the damage parameters D_1 and D_2 , we assume that the original specimens of the analyzed alloy are defect-free and can be characterized by the elasticity modulus E_0 or, after the corresponding number of AB cycles, by the moduli E .

Table 2
Elasticity Modulus E and Anisotropy Factor η after Alternating Bending
of the Sheets of ZE10 Alloy

Angle with RD, deg	No. of cycles of alternating bending									
	0		0.5		1		3		5	
	E , GPa	η , %	E , GPa	η , %	E , GPa	η , %	E , GPa	η , %	E , GPa	η , %
0	46.3		46		45.8		45		44.8	
15	44.3		44		43.8		43.5		43.7	
30	43.5		43.1		43		43.1		42.8	
45	43.1	7.4	43	7.0	42.8	7.0	42.7	5.9	42.5	5.4
60	43.3		43.2		43		42.5		42.5	
75	43.6		43.5		43.1		43		42.8	
90	43.9		43.8		43		43.3		43.3	
Mean value	44.0	7.4	43.8	7.0	43.5	7.0	43.3	5.9	43.2	5.4

Table 3
Damage Parameters D_1 and Anisotropy Factors η after Alternating
Bending of Sheets of the ZE10 Alloy

Angle with RD, deg	No. of cycles of alternating bending									
	0		0.5		1		3		5	
	$D_1 = (E - E_0)/E_0$	η	D_1	η	D_1	η	D_1	η	D_1	η
0			0.65		1.08		2.81		3.24	
15			0.68		1.13		1.81		1.35	
30			0.92		0.69		0.92		1.61	
45	0	0	0.23	303.7	0.46	195.9	0.93	142.0	1.39	132.7
60			0.23		1.39		1.85		1.85	
75			0.23		1.15		1.38		1.83	
90			0.23		2.05		1.37		1.37	
Mean value	0	0	0.45	303.7	1.14	195.9	1.59	142.0	1.82	132.7

Table 4
Damage Parameters D_2 and Anisotropy Factors η after Alternating
Bending of the Sheets of ZE10 Alloy

Angle with RD, deg	No. of cycles of alternating bending									
	0		0.5		1		3		5	
	$D_2 =$ $1 - (E/E_0)^{1/2}$	η	D_2	η	D_2	η	D_2	η	D_2	η
0			0.32		0.54		1.41		1.63	
15			0.34		0.57		0.91		0.68	
30			0.46		0.35		0.58		0.81	
45	0	0	0.12	304.4	0.23	195.5	0.58	145.3	0.705	133.8
60			0.12		0.70		0.93		0.93	
75			0.11		0.58		0.46		0.929	
90			0.11		1.03		0.69		0.69	
Mean value	0	0	0.23	304.4	0.57	195.5	0.80	145.3	0.91	133.8

The damage parameters D_1 and D_2 given by relations (2) and (3), respectively, are presented in Tables 3 and 4. It is easy to see that these parameters are also anisotropic. The maximal values of the parameters (303.7% and 304.3% for D_1 and D_2 , respectively) are observed after 0.5 AB cycle. As the number of AB cycles increases, their anisotropy becomes weaker. The minimal values (132.7% and 133.8% for D_1 and D_2 , respectively) are observed after 5 AB cycles.

The damage parameters averaged over all directions of sheets, namely, D_1^{av} and D_2^{av} , increase with the number of AB cycles (Tables 3 and 4). Our analysis reveals significant correlations between the damage parameters D_1^{av} and D_2^{av} averaged over all directions in the sheets of the analyzed alloy, on the one hand, and the number of AB cycles, on the other hand. The corresponding regression equations and reliability indices of the approximation R^2 take the form

$$D_1^{\text{av}} = -0.11n^2 + 0.87n + 0.10, \quad R^2 = 0.95, \quad (7)$$

$$D_2^{\text{av}} = -0.06n^2 + 0.44n + 0.05, \quad R^2 = 0.95. \quad (8)$$

The results of mechanical tests are presented in Tables 5–7. In this case, we observe the anisotropy of ultimate strength, yield point, and relative elongation both in the original sheets of the investigated alloy and after its alternating bending. Thus, for the ultimate strength of the original sheet, the maximal value of the anisotropy factor η is 13.9%. As the number of AB cycles increases, the value of η decreases and reaches its minimal value (9.4%) after 3 AB cycles. After 5 AB cycles, the anisotropy factor increases to 12.1%.

Table 5
Ultimate Strength σ_u and Anisotropy Factor η After the Alternating
Bending of the Sheets of ZE10 Alloy

Angle with RD, deg	No. of cycles of alternating bending									
	0		0.5		1		3		5	
	σ_u , MPa	η , %	σ_u , MPa	η , %	σ_u , MPa	η , %	σ_u , MPa	η , %	σ_u , MPa	η , %
0	246		250		252		256		250	
45	231	13.9	219	13.1	219	12	221	9.4	229	12.1
90	216		221		225		234		223	
Mean value	231.2	13.9	230	13.1	232	12	237	9.4	234	12.1

Table 6
Yield Point $\sigma_{0.2}$ and Anisotropy Factor η After the Alternating
Bending of the Sheets of the ZE10 Alloy

Angle with RD, deg	No. of cycles of alternating bending									
	0		0.5		1		3		5	
	$\sigma_{0.2}$, MPa	η , %	$\sigma_{0.2}$, MPa	η , %	$\sigma_{0.2}$, MPa	η , %	$\sigma_{0.2}$, MPa	η , %	$\sigma_{0.2}$, MPa	η , %
0	174		174		102		89		115	
45	132	90.2	99	97.7	88	14.6	100	12.4	89	29.2
90	91.5		88		89		96		90	
Mean value	132.5	90.2	120.3	97.7	93	14.6	95	12.4	98	29.2

The ultimate strength averaged over all directions in the sheet increases from 231.2 MPa (in the original sheet) to the maximal value 237 MPa (after 3 AB cycles). However, after 5 AB cycles, it decreases to 234 MPa (Table 5).

The yield point of original sheet of the analyzed alloy is characterized by significant anisotropy (90%). Because of alternating bending, as the number of cycles increases, the anisotropy of the yield point becomes much weaker and the anisotropy factor takes the minimal value (12.4% after 3 AB cycles). After 5 AB cycles, the anisotropy factor again increases up to 29.2%. The yield point averaged over all directions in the sheets decreases from 120 MPa in the original sheet down to 98 MPa as the number of AB cycles increases from 0 to 5 (Table 6).

Table 7
Relative Elongation $\Delta l/l$ and Anisotropy Factor η After the Alternating
Bending of the Sheets of the ZE10 Alloy

Angle with RD, deg	No. of cycles of alternating bending									
	0		0.5		1		3		5	
	$\Delta l/l$	η	$\Delta l/l$	η	$\Delta l/l$	η	$\Delta l/l$	η	$\Delta l/l$	η
	%									
0	23.4		21.0		20.5		19.1		29.0	
45	28.0	42.7	36.1	71.9	19.1	90.5	35.6	43.8	25.0	20.8
90	33.4		32.6		36.4		20.0		24.0	
Mean value	28.3	42.7	29.0	71.9	25.3	90.5	24.9	43.8	26.0	20.8

The anisotropy of relative elongation of the investigated alloy increases from 42.7% in the original sheet to the maximal value (90.5%) attained after 1 AB cycle. As the number of AB cycles increases, the value of $\Delta l/l$ decreases to its minimum value (20.8% after 5 AB cycles). The value of $(\Delta l/l)_{av}$ averaged over all directions in sheets is maximal (29%) after 0.5 cycle of alternating bending, then it reaches the minimal level 24.9% after 3 AB cycles but, after 5 cycles, again increases to 26% (Table 7).

The results of our analysis show that there exists a correlation between the values of ultimate strength σ_u^{av} , conventional yield point $\sigma_{0.2}^{av}$, and relative elongation $(\Delta l/l)_{av}$ averaged over the directions, on the one hand, and the number of AB cycles, on the other hand. The corresponding regression equations and the reliability factors of approximation are given by the formulas

$$\sigma_u^{av} = -0.57n^2 + 3.77n + 229.67, \quad R^2 = 0.78, \quad (9)$$

$$\sigma_{0.2}^{av} = 4.00n^2 - 35.67n + 128.19, \quad R^2 = 0.78, \quad (10)$$

$$\left(\frac{\Delta l}{l}\right)_{av} = 0.42n^2 - 2.63n + 28.70, \quad R^2 = 0.71. \quad (11)$$

It is known that one of the main causes of formation of the anisotropy of physicomechanical properties of polycrystalline metal materials is their crystallographic texture formed as a result of deformation. As already indicated, the Kearns texture parameters are often used for the quantitative evaluation of the textures of hexagonal materials [23].

We now analyze the anisotropy of characteristics and their changes (Tables 2–7) in connection with the crystallographic texture expressed via the Kearns texture parameters f_{ND} (for the original sheet) and f_{ND}^{av} averaged over two sides of the sheets after the corresponding number of AB cycles (Table 1). The results of our analyses demonstrate that there exist correlations between the moduli of elasticity, damage parameters, and mechanical characteristics averaged over all directions in the sheets, on the one hand, and the indicated Kearns

texture parameters, on the other hand. The corresponding regression equations and the reliability indices of approximation are given by the relations

$$E_{av} = -2149.3(f_{ND}^{av})^2 + 14440f_{ND}^{av} - 198.5, \quad R^2 = 0.83, \quad (12)$$

$$D_1^{av} = 4901(f_{ND}^{av})^2 - 3292.6f_{ND}^{av} + 552.9, \quad R^2 = 0.83, \quad (13)$$

$$D_2^{av} = 2450.8(f_{ND}^{av})^2 - 1646.6f_{ND}^{av} + 276.5, \quad R^2 = 0.83, \quad (14)$$

$$\sigma_B^{av} = 45497(f_{ND}^{av})^2 - 30092f_{ND}^{av} + 5209.9, \quad R^2 = 0.98, \quad (15)$$

$$\sigma_{0.2}^{av} = -79175(f_{ND}^{av})^2 + 53723f_{ND}^{av} - 8980.5, \quad R^2 = 0.83, \quad (16)$$

$$\left(\frac{\Delta l}{l}\right)_{av} = -20937(f_{ND}^{av})^2 + 13902f_{ND}^{av} - 2278, \quad R^2 = 0.76. \quad (17)$$

CONCLUSIONS

The texture of the original sheet of ZE10 alloy is characterized by a broad scattering of the elevated pole density of normals to the basis planes in the TD with the maximal angle of deviation from the DN equal to 90° and the intermediate maxima of deviations of the hexagonal prism from the DN both to the side of the TD by 40° and to the side of the RD by 40° , unlike the textures usually formed in Mg, Ti, and Zr. We revealed the anisotropy of the modulus of elasticity, damage parameters, ultimate strength, yield point, and relative elongation both in the original sheet of ZE10 alloy and after alternating bending. As the number of AB cycles increases, the anisotropy of the investigated characteristics becomes weaker. It is shown that the moduli of elasticity averaged over all directions in sheets decrease, whereas the damage parameters, ultimate strength, yield point, and relative elongation, on the contrary, increase as the number of cycles of alternating bending increase from 0 to 5. The variations of the modulus of elasticity, damage parameters, and mechanical properties in the uniaxial tensile tests are mainly caused by the crystallographic textures of the sheets of ZE10 alloy formed in the course of thermomechanical treatment and subsequent alternating bending.

The accumulated results can be used for the development of the technology of manufacturing of thin sheets of magnesium alloys with additions of zinc, zirconium, and rare-earth metals with improved characteristics of form changes and the minimal anisotropy of the mechanical characteristics.

REFERENCES

1. Z. Yang, J. P. Li, J. X. Zhang, G. W. Lorimer, and J. Robson, "Review on research and development of magnesium alloys," *Acta Metallurg. Sinica*, **21**, No. 5, 313–328 (2008); URL: <https://www.sciencedirect.com/science/article/abs/pii/S100671910860054X>.
2. R. Li, F. Pan, B. Jiang, H. Dong, and Q. Yang, "Effect of Li addition on the mechanical behavior and texture of the as-extruded AZ31 magnesium alloy," *Mater. Sci. Eng., Ser.: A*, **562**, No. 1, 33–38 (2013); URL: <http://dx.doi.org/10.1016/j.msea.2012.11.032>.
3. K. K. Alaneme and E. A. Okoleta, "Enhancing plastic deformability of Mg and its alloys—A review of traditional and nascent developments," *J. Magnesium Alloy*, **5**, No. 4, 460–475 (2017); URL: <https://doi.org/10.1016/j.jma.2017.11.001>.
4. R. K. Mishra, A. K. Gupta, P. R. Rao, A. K. Sachdev, A. M. Kumar, and A. A. Luo, "Influence of cerium on the texture and ductility of magnesium extrusions," *Scripta Mater.*, **59**, No. 5, 562–565 (2008); URL: <https://www.sciencedirect.com/science/article/pii/S135964620800362X>.

5. L. W. F. Mackenzie and M. O. Pekguleryuz, "The recrystallization and texture of magnesium–zinc–cerium alloys," *Scripta Mater.*, **59**, No. 6, 665–668. (2008); URL: <https://www.sciencedirect.com/science/article/pii/S1359646208003874>.
6. N. Stanford and M. Barnett, "Effect of composition on the texture and deformation behavior of wrought Mg alloys," *Scripta Mater.*, **58**, No. 3, 179–182 (2008); URL: <https://www.sciencedirect.com/science/article/pii/S1359646207006938>.
7. J. D. Robson, "Critical assessment 9: Wrought magnesium alloys," *Mater. Sci. Technol.*, **31**, No. 3, 257–264 (2015); URL: <https://doi.org/10.1179/1743284714Y.0000000683>.
8. *Methods of Leveling Sheet Metal*, ARKU Magazine; URL: <https://www.arku.com/us/arku-magazine/detail/sheet-metal-leveling-methods-us/>.
9. N. M. Shkatulyak, V. V. Usov, N. A. Volchok, A. A. Bryukhanov, S. V. San'kova, M. Rodman, M. Shaper, and C. Klose, "Effect of reverse bending on texture, structure, and mechanical properties of sheets of magnesium alloys with zinc and zirconium," *Phys. Metals Metallogr.*, **115**, No. 6, 609–616 (2014); URL: <https://link.springer.com/article/10.1134/S0031918X1406012X>.
10. L. M. Kachanov, *Foundations of Fracture Mechanics* [in Russian], Nauka, Moscow (1974).
11. Yu. N. Rabotnov, *Selected Works* [in Russian], Nauka, Moscow (1991).
12. J. Lemaitre and R. Desmorat, "Anisotropic damage law of evolution," *Eur. J. Mech. A/Solids*, **19**, No. 2, 187–208 (2000); URL: <https://www.sciencedirect.com/science/article/pii/S0997753800001613>.
13. N. R. Hansen and H. L. Schreyer, "A thermodynamically consistent framework for theories of elastoplasticity coupled with damage," *Int. J. Solid. Struct.*, **31**, No. 3, 359–389 (1994); URL: [https://doi.org/10.1016/0020-7683\(94\)90112-0](https://doi.org/10.1016/0020-7683(94)90112-0).
14. C. L. Chow and J. Wang, "An anisotropic theory of elasticity for continuum damage mechanics," *Int. J. Fract.*, **33**, No. 1, 3–16 (1987); URL: <https://link.springer.com/article/10.1007/BF00034895>.
15. M. Bobyr O. Khalimon, and O. Bondarets, "Phenomenological damage models of anisotropic structural materials," *J. Mech. Eng. NTUU "Kyiv Polytechnic Institute."* No. 67, 5–13 (2013); URL: http://nbuv.gov.ua/UJRN/VKPI_mash_2013_67_3.
16. V. V. Usov and N. M. Shkatulyak, "Fractal nature of the dislocation structure of low-alloyed steel after controlled rolling," *Russ. Phys. J.*, **47**, No. 11, 1139–1146 (2004); URL: <https://link.springer.com/article/10.1007/s11182-005-0044-y>.
17. *WIPO Patent Application WO/2011/146970*; URL: <http://www.sumobrain.com/patents/wipo/Magnesium-based-alloy-wrought-applications/WO2011146970A1.html>.
18. P. R. Morris, "Reducing the effects of nonuniform pole distribution in inverse pole figure studies," *J. Appl. Phys.*, **30**, No. 4, 595–596 (1959); URL: <https://doi.org/10.1063/1.1702413>.
19. J. J. Kearns, *Thermal Expansion and Preferred Orientation in Zircaloy*; URL: <https://ntrl.ntis.gov/NTRL/dashboard/searchResults/titleDetail/WAPDTM472.xhtml>.
20. Ya. D. Vishnyakov, A. A. Babareko, S. A. Vladimirov, and I. V. Egiz, *Theory of Texture Formation in Metals and Alloys* [in Russian], Nauka, Moscow (1979).
21. L. I. Mirkin, *Handbook on X-ray Diffraction Analysis of Polycrystals* [in Russian], Fizmatgiz, Moscow (1961).
22. Y. Liu, W. Li, and Y. Li, "Microstructure and mechanical properties of ZE10 magnesium alloy prepared by equal channel angular pressing," *Int. J. Minerals, Metallurgy, Mater.*, **16**, No. 5, 559–563 (2009); URL: [https://doi.org/10.1016/S1674-4799\(09\)60096-0](https://doi.org/10.1016/S1674-4799(09)60096-0).
23. V. Grytsyna, D. Malykhin, T. Yurkova, K. Kovtun, T. Chernyayeva, G. Kovtun, I. Tantsura, and V. Voyevodin, "On structural aspects of texture changes during rolling of Zr–2.5% Nb alloy," *East Eur. J. Phys.*, No. 3, 38–45 (2019); URL: <https://doi.org/10.26565/2312-4334-2019-3-05>.